NOTE:

The following pages are the supporting information as submitted to PNAS, which differ in numbering from the published text.

The numbering conversions are as follows:

As submitted	As published
Figure S1	Figure 5
Figure S2	Figure 6
Figure S3	Figure 7
Figure S4	Figure 8
Figure S5	Figure 9
Figure S6	Figure 10
Table S1	Table 1

The supporting information is officially found on the PNAS website at:
http://www.pnas.org/cgi/content/full/0403884101/DC1

Supplementary Materials:

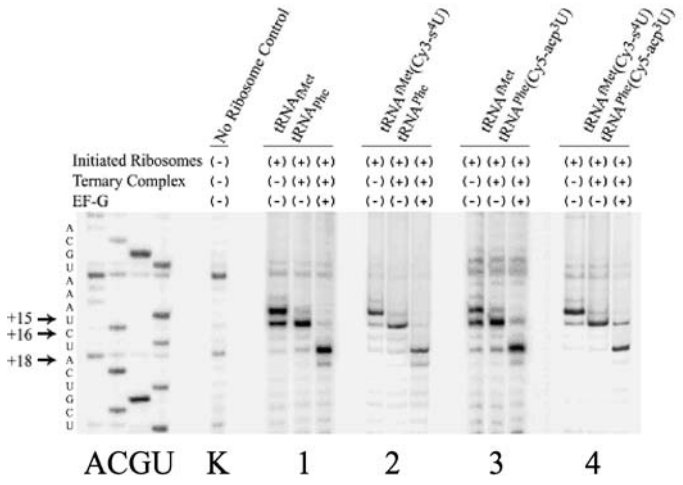

Figure S1: Toeprinting analysis using purified translation components. Toeprinting assays were performed as reported (1),(2) with the following modifications. 70S initiation complexes were prepared by initiating 70S ribosomes on a gene32-derived mRNA with fMet-tRNA^{fMet} (or fMet-tRNA^{fMet}(Cy3-$_{4s}$U)) as reported in Materials and Methods for single molecule studies. Phe-tRNA^{Phe} (or Phe-tRNA^{Phe}(Cy5-Acp3)) was delivered in a ternary complex with EF-Tu(GTP) prepared as described in Materials and Methods for single molecule studies. 70S initiation complexes (250 nM final concentration) were incubated with ternary complex (500 nM final concentration) in the absence and presence of EF-G(GTP) (500 nM final concentration) for 5 min at 25 ºC. Reactions were quenched by the additiof viomycin to a final concentration of 1 mM and primer extended by reverse transcription for 15 min at 37 ºC as described (3). Reverse transcription is blocked when polymerase encounters the ribosome. Thus, the length of oligonucleotide products generated by the reaction reports on where the ribosome is positioned on mRNA and is a sensitive indicator of the efficiencies of tRNA delivery to the A site and translocation (4). In Fig. S1, sequencing of the gene32-derived mRNA is shown in the four lanes on the left and the lane labeled K shows primer extension of the free gene32-derived mRNA.

The four panels on the right show toeprinting data using purified elongation factors and the four combinations of natural and fluorescently-labeled tRNA substrates. Panel 1: fMet-tRNA^{fMet} and Phe-tRNA^{Phe}; Panel 2: fMet-tRNA^{fMet}(Cy3-s^{4}U) and Phe-tRNA^{Phe}; Panel 3: fMet-tRNA^{fMet} and Phe-tRNA^{Phe}(Cy5-acp^{3}U) and Panel 4: fmet-tRNA^{fMet}(Cy3-s^{4}U) and Phe-tRNA^{Phe}(Cy5-acp^{3}U). Within each panel is shown a control reaction revealing the toeprint from ribosomes initiated on gene32-derived mRNA template (left lane), the same reaction following enzymatic delivery of Phe-tRNA^{Phe} (middle lane) and following enzymatic delivery of Phe-tRNA^{Phe} and EF-G(GTP) (right lane). Quantitative phosphorimage analysis of the toeprinting products shows that accommodation and translocation are ~90% efficient using any combination of substrates.

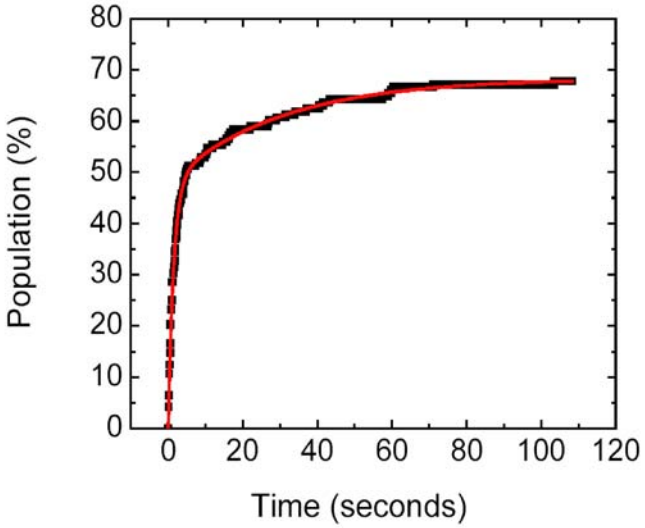

Figure S2: FRET arrival time plot. The percentage of surface-immobilized ribosome complexes carrying fMet-tRNA^{fMet}(Cy3-s^{4}U) in the P site that achieve an observable FRET signal (≥0.25) upon stopped-flow delivery of EF-Tu(GTP)Phe-tRNA^{Phe}(Cy5-acp^{3}U) is plotted *vs.* the time at which FRET appears. FRET is observed for the majority of ribosome complexes (~70%). The data are best described by a double exponential: $A - B\exp(-t/\tau_1) - C\exp(-t/\tau_2)$ where B and τ_1 represent the amplitude and decay time of the "burst" component of the curve, respectively. C and τ_2 represent the slower component. The fitting parameters were: A = 68, B = 47 (70%), τ_1 = 1.51 ± 0.01 s, C = 20 (30%) and τ_2 = 30.29 ± 0.31 s.

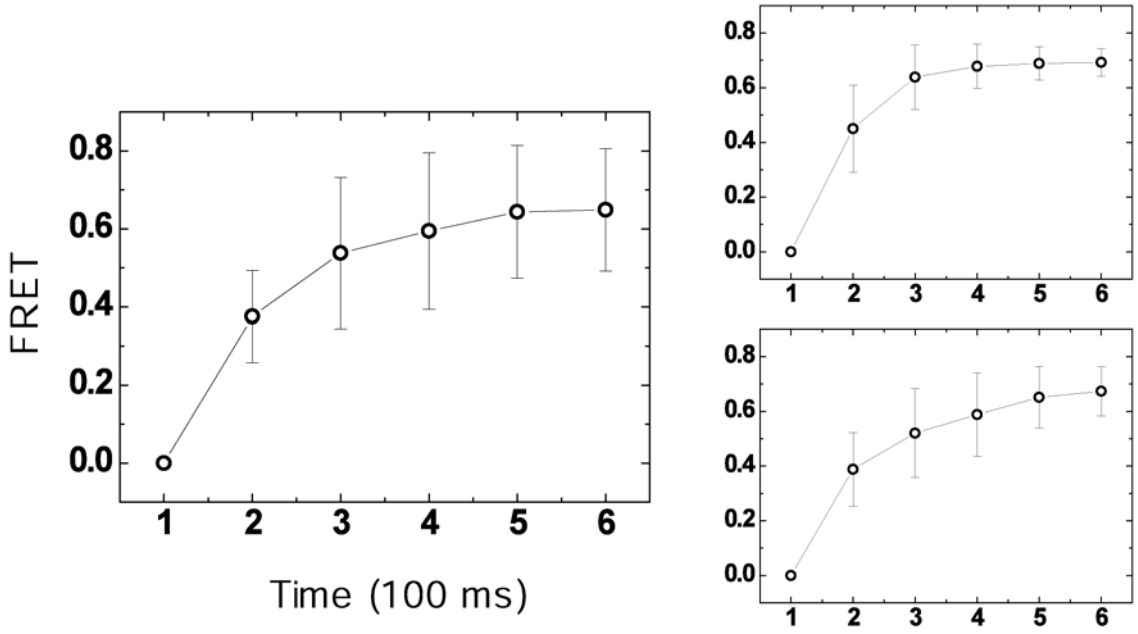

Figure S3: Monte Carlo simulation of tRNA accommodation. The smFRET signal increases upon delivery of EF-Tu(GTP)Phe-tRNA^{Phe} (Cy5-acp^{3}U) to surface-immobilized ribosome complexes initiated with fMet-tRNA^{fMet} (Cy3-s^{4}U) in the P site and a UUU codon in the A site. The change in FRET for each individual molecule was recorded for the first five data points following appearance of FRET signal ≥0.25 and plotted (left panel). The gradual increase in FRET observed over the first three data points is consistent with the existence of one or more intermediate state from the point of initial binding to complete aa-tRNA accommodation. Monte Carlo simulations on an ensemble of molecules were performed with the assumption that there is a single intermediate at a FRET value of 0.35 and a final FRET value of 0.7. Plots of the simulations, shown in the right panels assume that the intermediate has a lifetime of 100 ms (upper panel) and 200 ms (lower panel).

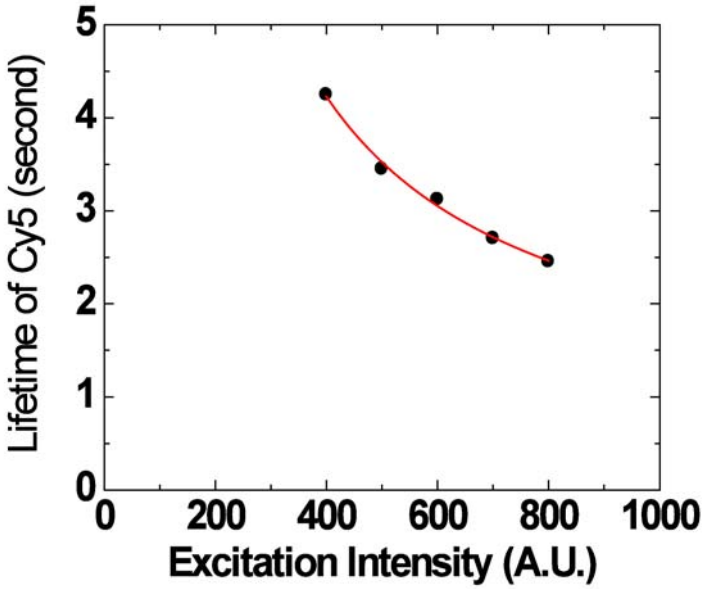

Figure S4. Cy5 fluorescence lifetime analysis. The lifetime of Cy5 between dark states of zero FRET value ("blinking events") was measured as a function of excitation intensity of the 532 nm laser. The lifetime of Cy5 in states with a FRET value ≥0.25 decreases, or Cy5 drops to the zero FRET state more frequently, as the excitation intensity is increased. Assuming that the observed blinking is light-induced, the lifetime is fitted to a+b/I, where I is the excitation intensity and a and b are fitting parameters. The time spent in this dark state has a single exponential lifetime of 1.4 seconds at typical illuminating conditions. More detailed analysis shows that the time Cy5 spends in the fluorescent state until it "blinks" is similar to the non-recovering photobleaching time in direct excitation by a 635 nm laser.

These observations suggest that fluctuations to the zero FRET state are not due to changes in distance between the tRNA elbows. We believe that "blinking" is an intrinsic photo-physical property of the Cy5 dye and its interactions with the local micro-environment.

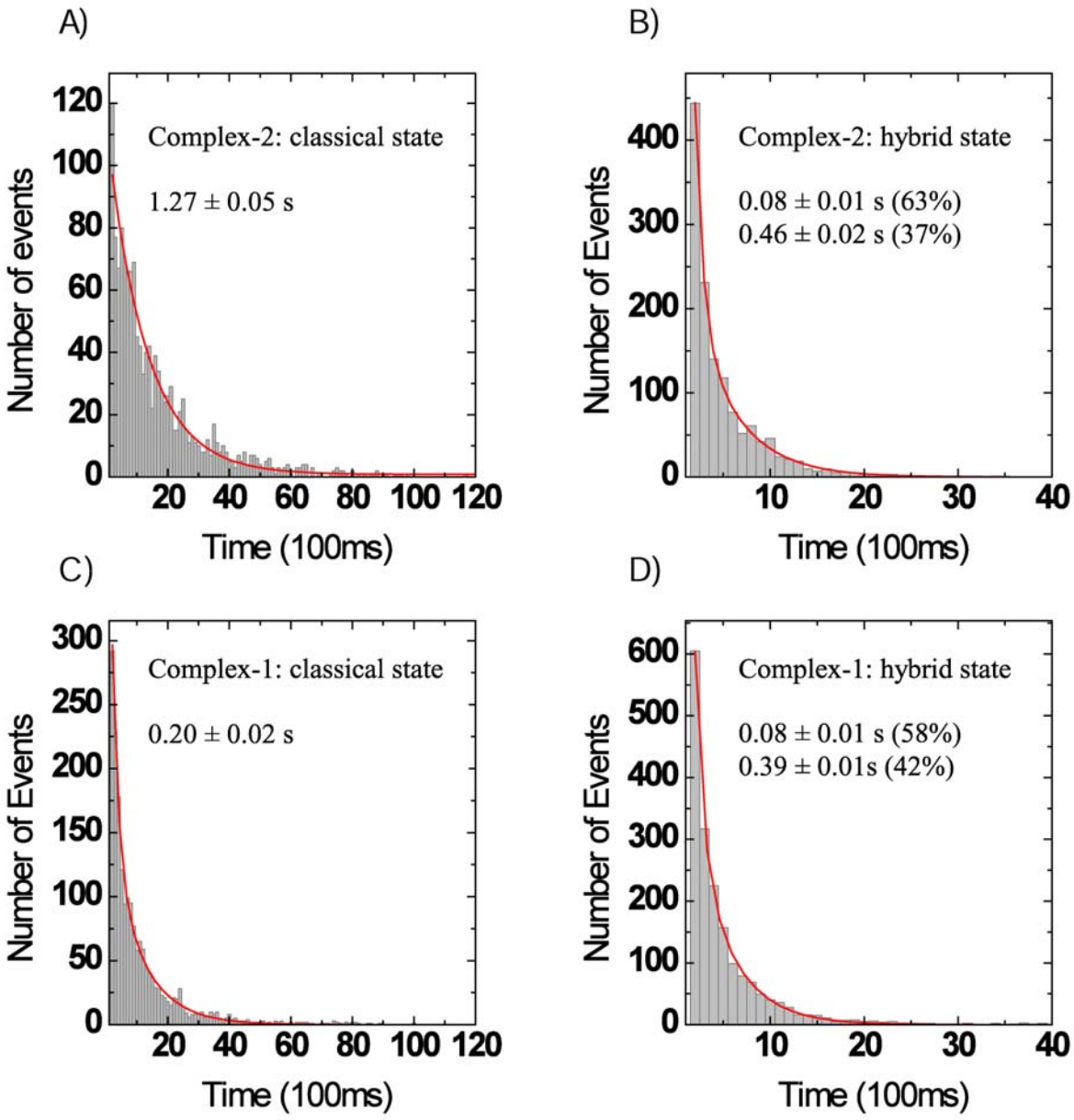

Figure S5: Lifetime analysis of classical and hybrid states. EF-Tu(GTP)Phe-tRNA^{Phe}(Cy5-acp^{3}U) was delivered to surface-immobilized ribosomes carrying either fMet-tRNA^{fMet}(Cy3-s^{4}U) or OH-tRNA^{fMet}(Cy3-s^{4}U) in the P site (complex-1 and -2, respectively). In the present analysis, EF-Tu(GTP)Phe-tRNA^{Phe}(Cy5-acp^{3}U) free in solution was removed after a 5 minute incubation and the Cy3 excitation power was increased; both changes improve the signal-to-noise of the

lifetime analysis. The observed fluctuations arise from tRNAs stably bound to the ribosome after accommodation. In both complexes, fluctuations are observed between 0.75 and 0.45 FRET states (assigned as classical- and hybrid-state tRNA configurations, respectively). In this analysis, the threshold between 0.75 and 0.45 FRET states was set to 0.55 and 0.58 for complex-1 and -2, respectively and the lifetime analysis was performed on data first subjected to a 2-point rolling averaging of donor and acceptor signals. Histograms of the times spent in the classical and hybrid states were fit to single or double exponential decay functions using a nonlinear least squares fitting algorithm (Origin, Microcal). Typical smFRET traces of both data sets are shown in the insert below.

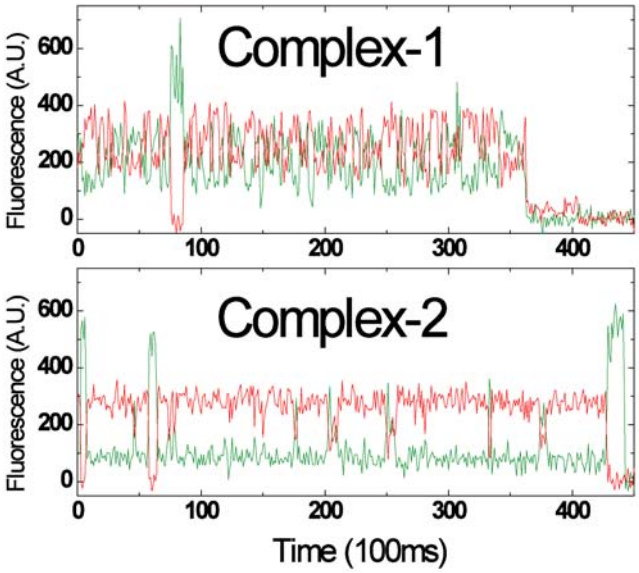

For complex-2, the lifetime of classical state (A) fits to a single exponential decay with a lifetime of 1.27 ± 0.05 s. For complex-1, the classical state lifetime (C) fits to a double exponential decay where 64% of the population has a lifetime of 1.03 ± 0.05 s and the remaining 36% with 0.20 ± 0.02 s. The longer lifetime can be forced to 1.27 s, the same as the lifetime of classical state in complex-2, without significantly changing the goodness of the fit χ^2 (12.1 to

13.1) or the shorter lifetime (0.2 to 0.25 s). Therefore, we conclude that the longer lifetime component (64%) represents the population of ribosomes carrying deacylated-tRNA in the P site. The hybrid state shows two decay lifetimes, 0.08 ± 0.01 s (63%) and 0.46 ± 0.02 s (37%) for complex-2 (B) and 0.08 ± 0.01 s (58%) and 0.39 ± 0.01s (42%) for complex-1 (D). Although the times and ratios for the hybrid state are somewhat different for the two complexes, this effect is minor compared to the change in classical state kinetics. At present, we do not know the origin of the double-exponential kinetics of the hybrid state. Using this lifetime data, we calculate that the hybrid state is occupied 14% of the time when peptide bond formation is blocked and 51% of the time when peptide bond formation is allowed.

Also from the lifetime analysis, the free energy of activation ($\Delta^{\ddagger}G$) required for the classical-hybrid transition is lowered from 76 kJ mol^{-1} for complex-2 to 71.8 kJ mol^{-1} for complex-1 as a result of destabilized binding of peptidyl tRNA in the A site according to the equation: $\Delta^{\ddagger}G = -RT\ln\left(\frac{hk}{k_B T}\right)$ where k is the rate constant, R gas constant, T temperature, k_B Boltzmann constant, and h Planck constant.

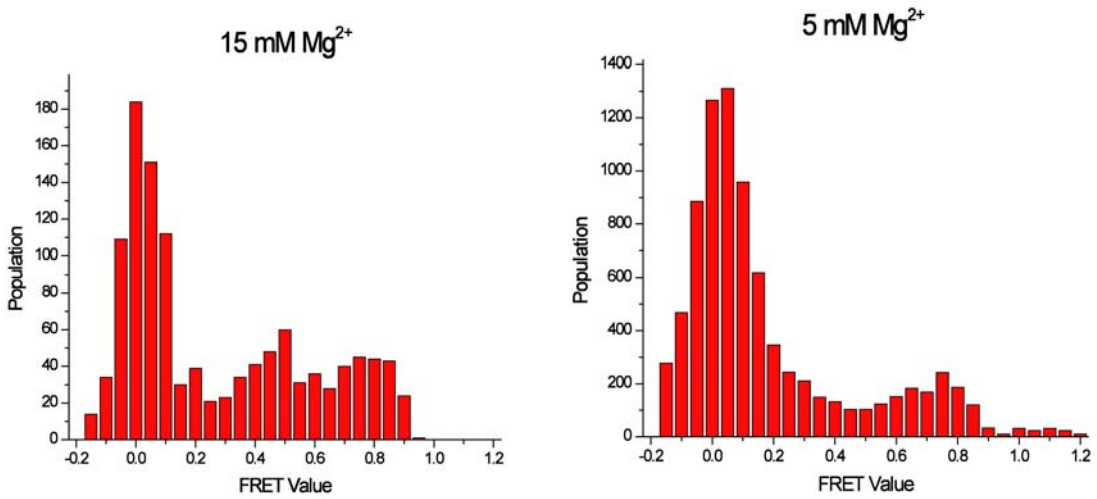

Figure S6. The Mg^{2+} dependence of FRET populations after peptide bond formation. At 5 mM Mg^{2+}, the two FRET values become less well defined and the peaks in the population histograms are no longer clearly resolvable. This result is consistent with averaging due to an increased rate of interconversion between the two FRET states at lower Mg^{2+} so that the lifetime of the two FRET states is comparable to, or faster than, the video frame collection rate (10 s^{-1}). In support of this view, data acquired at 5 ms integration time on a confocal microscope reveals that, at 5 mM Mg^{2+}, FRET fluctuations take place on a time scale faster than 100 ms (data not shown).

A)

Environment of Cy3 Dye	Solution		Surface	
	r	τ_r (ns)	r	τ_r (ns)
Cy3	0.21	0.33	—	—
fMet-tRNA^{fMet}(Cy3-s^{4}U)	0.30	0.90	—	—
P-site Bound fMet-tRNA^{fMet}(Cy3-s^{4}U)	0.29	0.79	0.29	0.79
P-site Bound fMet-tRNA^{fMet}(Cy3-s^{4}U) + A-site Bound Phe-tRNA^{Phe}	—	—	0.30	0.90
P-site Bound fMet-tRNA^{fMet}(Cy3-s^{4}U) + A-site Bound Phe-tRNA^{Phe} + EF-G	—	—	0.29	0.79

B)

Environment of Cy5 Dye	Solution		Surface	
	r	τ_r (ns)	r	τ_r (ns)
Cy5	0.14	0.54	—	—
Phe-tRNA^{Phe}(Cy5-acp^{3}U)	0.15	0.60	—	—
P-site Bound fMet-tRNA^{fMet} + A-site Bound Phe-tRNA^{Phe}(Cy5-acp^{3}U)	—	—	0.25	1.67
P-site Bound fMet-tRNA^{fMet} + A-site Bound Phe-tRNA^{Phe}(Cy5-acp^{3}U) + EF-G	—	—	0.25	1.67

Table S1. Fluorescence anisotropy is defined by $r = \frac{I_{\parallel} - I_{\perp}}{I_{\parallel} + 2I_{\perp}}$, where $I_{\parallel}$ and $I_{\perp}$ are the fluorescence emission components parallel and perpendicular to the polarization axis of the linearly polarized excitation. Using two polarizing cube beamsplitters, $I_{\parallel}$ and $I_{\perp}$ can be spatially separated and simultaneously recorded by the same camera. Assuming that only the rotational motion of a dye randomizes the polarization of fluorescence emission, r can be expressed with

the fluorescence lifetime (τ_f) and the rotational correlation time (τ_r) of a dye as: $r = \frac{0.4}{1+\tau_f/\tau_r}$.

We measured r for Cy3 dyes free in solution and on fMet-tRNA^{fMet}(Cy3-s^{4}U) free in solution and on fMet-tRNA^{fMet}(Cy3-s^{4}U) within the P site of 70S initiation complexes both in solution and immobilized on quartz surfaces. Additionally, r was measured for fMet-tRNA^{fMet}(Cy3-s^{4}U) within the P site of surface-immobilized 70S initiation complexes upon delivery, in a manner identical to smFRET experiments, of Phe-tRNA^{Phe} in complex with EF-Tu(GTP) in the presence and absence of EF-G(GTP). The resulting values of r and τ_r, calculated assuming τ_f of Cy3 to be 0.3 ns (Amersham Biosciences), are presented in Table S1. Similar measurements were done for the Cy5 dye labels. The rotational correlation time of the ribosome is reported to be ~1 μs (5).

Anisotropy data measure the rotation during the excited state lifetime of the dyes (< 300 ps for Cy3 and ~1 nsec for Cy5) while the FRET data is sensitive to the average angular orientations averaged over 100 milliseconds. Non-zero r-values may simply indicate that the rotational relaxation is partially hindered on the nanosecond time scale but is complete at the 100 millisecond time scale. Alternatively, a finite r-value could indicate that the attached dye molecule spends part of the time bound in a fixed orientation to the tRNA or the ribosome and part of the time in a freely rotating state.

The fact that the distance between the elbow labeling sites of the P/P and A/A bond tRNAs agree with the crystallographic distances suggests that the relative orientation of the donor and acceptor dyes are mostly freely rotating at the 100 milliscecond time scale. Thus, the observed FRET fluctuations, pre- and post-translocation, are probably due to changes in distance between the elbow regions of the tRNA molecules on the ribosome and not due to changes in the rotational freedom of the dyes.

References.

1. Hartz, D., McPheeters, D. S., Traut, R. & Gold, L. (1988) *Methods in Enzymology* **164,** 419-425.
2. Joseph, S. & Noller, H. F. (1998) *EMBO Journal* **17,** 3478-83.
3. Fredrick, K. & Noller, H. (2003) *SCIENCE* **300,** 1159-1162.
4. Studer, S. M., Feinberg, J. S. & Joseph, S. (2003) *Journal of Molecular Biology* **327,** 369-81.
5. Fairclough, R. H., Cantor, C. R., Wintermeyer, W. & Zachau, H. G. (1979) *Journal of Molecular Biology* **132,** 557-73.